RCA

LB-916

THE VARIATION OF CURRENT GAIN

WITH JUNCTION SHAPE

AND SURFACE RECOMBINATION

IN ALLOY TRANSISTORS

RADIO CORPORATION OF AMERICA
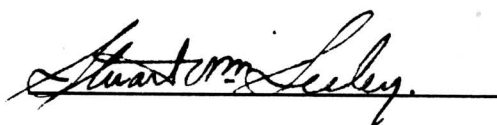# RCA LABORATORIES DIVISION
INDUSTRY SERVICE LABORATORY

RADIO CORPORATION OF AMERICA

RCA LABORATORIES DIVISION

INDUSTRY SERVICE LABORATORY

LB-916

The Variation of Current Gain

with Junction Shape and Surface Recombination

in Alloy Transistors

Approved

Stuart Wm. Seeley.

The Variation of Current Gain with Junction Shape and Surface Recombination in Alloy Transistors

Introduction

This bulletin presents an experimental and theoretical study of the effect on current gain of the size and shape of the p-n junctions, and of the surface recombination, in alloy transistors, such as the TA-153 described in *LB-868*. The experiments show that, on the average, the maximum current gain is attained when the collector area is several times the emitter area. The value of current gain is affected greatly by geometry and surface treatment, but is hardly affected at all by bulk recombination factors (lifetime) in the base. The known one-dimensional analyses of the junction transistor are not applicable for the convex junction shapes found in alloy units. A new calculation of the current gain for certain geometries is made herein, based on an electric analog solution to the diffusion equations in which surface recombination is taken as the predominant factor in minority carrier loss. If reasonable values of the surface recombination velocity s are chosen, agreement with the experiments is satisfactory.

By use of the theory, a new method of estimating surface recombination from simple measurements on transistors has been devised. This consists of measuring the ratio of current-gain factor, α_{ce}, in the normal connection, to α_{ce} with emitter and collector reversed. Use of a suitable calibration curve applicable to TA-153 units gives the value of s directly. Measurements on many TA-153 units yield values of s from 400 to 3000 cm/sec. A quantitative evaluation of the surface condition is thereby attained which may be useful for quality control.

Minority carriers suffer a transit-time path-length dispersion in a transistor structure with non-parallel junctions. This effect has been calculated for typical alloy junction shapes. The limitations on high-frequency performance imposed by the transit time effect will be significant only above 1 Mc/sec in a typical TA-153 structure. Other factors are more important in limiting high-frequency performance in this type.

Although this bulletin makes use of the p-n-p transistor as an example, the principles are equally applicable to n-p-n transistors.

General Discussion

The theories of junction transistor operation given in the literature[1,2] are limited in certain applications because of two important approximations: (1) one-dimensional geometry is assumed, (2) surface recombination is neglected or at best incorporated into a composite base lifetime. While it is true that for many transistors these approximations are not restrictive, some practical transistor designs violate them. In particular, alloy type junction transistors[3] may make questionable the interpretation of results based on infinite parallel plane geometry.

Since sectioned p-n-p alloy transistors (type TA-153) generally reveal convex junction shapes, a solution of the diffusion equations in three dimensions has been worked out which takes into account the geometrical effects. This solution is based on an analogy with current flow in a conducting sheet, under the assumption that surface recombination is the dominant factor in minority carrier loss. The results, which are obtained by plotting the hole flow vector field on a scale model, are compared with experiments on transistors made with various junction shapes. It will be shown that the departure from plane parallel geometry contributes to lowering the transistor current gain at d.c. and inserts a transit-time pathlength dispersion which may limit operation at high frequency. The influence of surface recombination velocity on these properties will be discussed. A method of estimating the surface recombination coefficient in the transistor structure will be demonstrated, based on the analogy solution.

Method of Solution

The collector-to-emitter input current gain α_{ce} is given by:

$$\alpha_{ce} = \alpha^* \beta \gamma \qquad (1)$$

where α^* is the intrinsic current gain of the collector junction, β is a survival factor which gives the ratio of minority carriers arriving at the collector to that released at the emitter and γ is the efficiency of emitter as an injector of minority carriers. For transistors not containing collector "hooks", α^* is generally taken as 1. γ is very close to unity for alloy transistors since $\sigma_{emitter} >> \sigma_{base}$ (see references 1-3). In this bulletin the concern shall be solely with the calculation of β. Since by assumption $\alpha^* = \gamma = 1$, $\alpha_{ce} = \beta$.

Minority carriers present in the base in small concentration in excess of the thermal equilibrium value obey certain differential equations. If, for example, the hole current in an n-type semiconductor is considered, the net current is composed of two parts. One part flows because of an electric field, since the holes are charged particles. The second part consists of a diffusion current which flows in the direction of lowest hole concentration in response to a concentration gradient. This flow is opposite in sign to the concentration gradient vector. The current flow vector also obeys an equation of continuity: the net change in the current flow in an elementary volume is accounted for by a change in the charge density with time due to flow out of the volume and by recombination of excess holes with electrons normally present in the volume. Mathematically, these two equations can be written:

$$\vec{I}_p = q p \mu_p \vec{E} - q D_p \nabla p \qquad (2)$$

$$\frac{1}{q} \nabla \cdot \vec{I}_p = -\frac{\partial p}{\partial t} - \frac{p - p_B}{\tau} \qquad (3)$$

Here p is the density, μ_p is the mobility, D_p is the diffusion coefficient, q is the charge, and τ is the lifetime of holes in the n-type material, p_B is the equilibrium concentration of holes, and E is the electric field.

These equations are subject to boundary conditions which define the hole density in the base at the emitter and collector. It is generally assumed that the electric field is negligible, i.e., diffusion currents dominate. It is also assumed that the hole density in the base is small compared to the electron density, so that all parameters such as conductivity, mobility, and lifetime are independent of injected carriers. Eqs. (2) and (3) can be

[1] Shockley, Sparks and Teal, "P-N Junction Transistors", *Phys. Rev.*, Vol. 83, p. 151, (1951).

[2] Steele, "Theory of Alpha for p-n-p Diffused Junction Transistors", *Proc. I.R.E.*, Vol. 40, p. 1424, (1952).

[3] LB-868, *Germanium p-n-p Junction Transistors*.

combined to give:

$$\frac{dp}{dt} = -\frac{p-p_B}{\tau} + D_p \nabla^2 p \qquad (4)$$

The steady-state equation is then

$$D \nabla^2 p - \frac{p-p_B}{\tau} = 0 \qquad (5)$$

For the one-dimensional case this can be readily solved (see references 1 and 2) and yields an equation for p(x) which can then be inserted into Eq. (2) to obtain I at emitter and collector. Then $\alpha = -\frac{\partial I_c}{\partial I_e}\Big|_{V_c}$ can be evaluated with the result

$$\alpha = \text{sech } W/L_p \qquad (6)$$

W is the width of the base layer and L_p is the diffusion length for holes ($L_p = \sqrt{D_p \tau}$).

The three-dimensional problem is far more difficult. A solution in closed form is possible only for restricted choices of the boundary conditions. However, experience has shown that transistor characteristics are not very sensitive to variation in τ provided τ is greater than a few microseconds, a condition easily achieved in practice. This will be discussed in detail later, but for the present simply assume that τ is sufficiently large in the base ($W/L_p \ll 1$) so that Eq. (5) becomes

$$\nabla^2 p = 0. \qquad (7)$$

Eq. 7 may also be written in terms of P, the excess hole density above the thermal equilibrium value ($P = p - p_B$):

$$\nabla^2 P = 0 \qquad (8)$$

This is a LaPlace equation solvable in two dimensions by the well-known engineering method of analogy to current flow in an electrolytic tank or conducting sheet. With the proper symmetry conditions, which will also be discussed later, the solution can be extended to three dimensions.

The equation which will be solved in the analogy is, of course, $\nabla^2 \varphi = 0$ so that electric potential φ is equivalent to excess hole density P. Eq. (8) must be solved subject to boundary conditions at emitter and collector. This means in the analogy that φ is fixed at φ_1 and φ_2 on these boundaries, or in other words, emitter

and collector become equipotential surfaces. An additional boundary condition, not required in the one-dimensional case, must be satisfied on all free surfaces of the germanium, namely that holes diffusing to the free surfaces disappear there by recombination, and thus constitute a hole current into the surface.[4] More precisely, the normal component of current density I into the surface is

$$\vec{I} = qP\vec{s} \qquad (9)$$

where s is the surface recombination velocity. s is the average velocity into the surface of holes present at the boundary. From Eq. (2), neglecting currents due to electric fields,

$$\vec{I} = -qD_p \nabla P \qquad (10)$$

so that

$$qPs = -qD_p \nabla P \qquad (11)$$

or

$$\frac{\nabla P}{P} = -\frac{s}{D_p} \qquad (12)$$

Therefore, provided s is constant over the surface, the boundary condition can also be stated as: the ratio of gradient P to P must be constant at all free surfaces.

Now consider the conducting sheet analogy. Let the edges (which correspond in two dimensions to surfaces in three dimensions) be bounded by a perfectly conducting boundary broken up into many segments of length a with
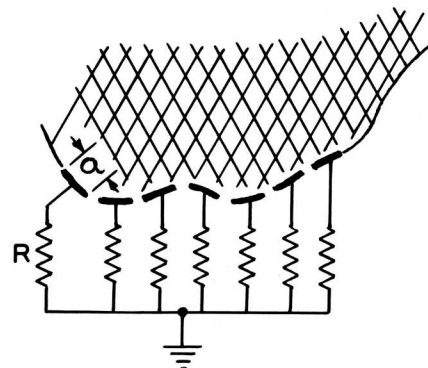

Fig. 1 — Boundary of a conducting region.

[4]Shockley, ELECTRONS AND HOLES IN SEMICONDUCTORS, Van Nostrand Co., p. 321.

each segment connected to ground through a resistance R as in Fig. 1. If the current density at the boundary is i then each segment collects current ia from the sheet, producing a voltage drop φ across R.

Then

$$ia = \frac{\varphi}{R} \qquad (13)$$

Within the sheet

$$\vec{i} = \frac{\vec{E}}{\rho} \qquad (14)$$

where ρ is the specific surface resistance of the sheet (ohms/square). Equating (13) and (14)

$$\frac{E}{\rho} = \frac{\varphi}{aR} \qquad (15)$$

Since

$$\vec{E} = -\nabla\varphi$$

$$\frac{\nabla\varphi}{\varphi} = -\frac{\rho}{aR} \qquad (16)$$

Comparison of Eqs. (12) and (16) shows that the analogy is complete if

$$\frac{\rho}{aR} = \frac{s}{D_p} \qquad (17)$$

For maximum accuracy of the solution near the boundaries the segment length a should be as small as possible. However, it is not necessary to assume that either s or a be constant over the whole free boundary; rather it is required that s does not change appreciably in a distance a so that Eq. (17) is obeyed. This will be utilized later to improve the accuracy with practical choice of a.

For convenience, the analogs are tabulated below.

The boundary conditions require that the emitter and collector be surfaces of constant excess hole density. No great error is introduced if it is assumed that φ at the collector = 0. This means that the collector is assumed to be perfect, collecting every hole which drifts into it from the semiconductor base. φ at the emitter is held fixed by a battery. With the proper boundary conditions established, the preparation of a rectilinear square map of equipotentials and field lines gives the required information about hole flow. While the discussion has been given for hole flow in n-type material it should be understood that the plotting method is equally applicable to electron flow in p-type material (n-p-n transistor) provided the proper value of D_n is used.

Conversion to Three Dimensions

The current carrying sheet analogy solves $\nabla^2\varphi = 0$ in two dimensions

$$\frac{\partial^2\varphi}{\partial x^2} + \frac{\partial^2\varphi}{\partial z^2} = 0 \qquad (18)$$

The problem to be solved is a three dimensional one:

$$\frac{\partial^2 P}{\partial r^2} + \frac{1}{r}\frac{\partial P}{\partial r} + \frac{1}{r^2}\frac{\partial^2 P}{\partial \theta^2} + \frac{\partial^2 P}{\partial z^2} = 0 \qquad (19)$$

With cylindrical symmetry, the third term in Eq. (19) is eliminated. In electrolytic tanks, this case can be solved by tipping the tank and using wedge-shaped electrodes as is done for axially symmetric electron lens problems.[5] In the present case, this is not convenient, nor, it turns out, is it necessary. The radii of emitter and collector electrodes are large compared to the spacing between them (along the z axis). In the map of P, $\partial P/\partial r$ is small near the origin where r is small. $\partial P/\partial r$ becomes appreciable only for r already large compared

Table I

Quantity in the map	Representation in the map	Quantity in the transistor	Representation in the transistor
Current	i	Current	I
Potential	φ	Excess hole density	P
$-\dfrac{\mathrm{grad}\ \varphi}{\varphi}$	ρ/aR	$-\dfrac{\mathrm{grad}\ P}{P}$	s/D_p

[5] Spangenberg, VACUUM TUBES, McGraw-Hill Co., N. Y., p. 80, (1948).

to W. Hence $1/r \, \partial P/\partial r$ is always small. The first and second derivatives of P were evaluated numerically for two geometrical cases. In a favorable case, $1/r \, \partial P/\partial r$ was less than 0.1 per cent of $\partial^2 P/\partial r^2$, while in a very unfavorable case $1/r \, \partial P/\partial r$ never exceeded 4 per cent of $\partial^2 P/\partial r^2$. Hence, it is justifiable to ignore the first derivative term. In the evaluation of total emitter and collector current the conversion from x in Eq. (18) to r in Eq. (19) is accomplished by numerically integrating over the electrode surfaces with a weight factor for r. This amounts to taking the area of an annular ring as $2\pi r \, dr$.

Justification for Neglecting Volume Recombination

For the one-dimensional case, β is given by Eq. (7). With W fixed at 1 mil, β is already 0.99 when $\tau = 10$ μsec. Germanium with bulk lifetime of 100 to 1000 μsec is generally used as transistor base material yielding $\beta = 0.999$ to 0.9999. As previously explained, γ is always very close to 1 because $\sigma_e >> \sigma_b$. Yet α_{ce} values of 0.95 – 0.98 are often found for alloy transistors. In a recent test of a large number of transistors made from crystals with measured bulk τ from 1 μsec to 1000 μsec, no correlation of α with bulk lifetime could be found. The possibility still exists that the alloying process reduces the bulk lifetime of the germanium within the base layer of the transistor. Then regardless of the quality of the starting material, the bulk lifetime may be short enough to effect β. Presumably this could be due to heat cycling during the alloying. Yet a piece of germanium subjected to a similar heat cycling treatment shows no adverse bulk lifetime effect. On the other hand, α is extremely sensitive to etching procedures after alloying. It seems reasonable to assume that the main loss of holes is through surface recombination.

It is clear that the validity of the plotting method depends on the assumption that holes are lost by surface recombination only. All other approximations made in the solution are of minor importance except for the choice of geometry. The extent to which the calculated results agree with experiment can be taken as a measure of the validity of neglecting bulk recombination.

Procedure

In order to illustrate the application of the principles described above, the procedure for plotting the hole flow and estimating β for a TA-153 type structure will be outlined. This procedure is applicable to other structures and has been utilized with appropriate changes in geometry and constants.

For this example junction geometry of the form shown in Fig. 2 is utilized. This is based on observation of sectioned TA-153 transistors. A convenient medium for field plotting is "Teledeltos" recording paper.[8] This paper has a specific resistance of 2000 ohms/square. Equipotential electrodes can be applied simply by painting with air-drying silver paste.
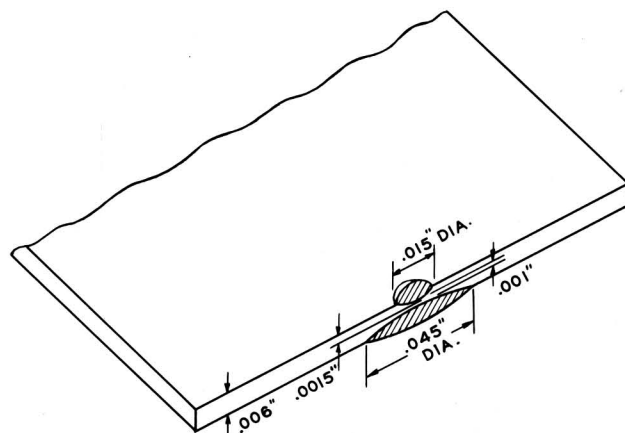

Fig. 2 – Dimensions of typical TA-153 p-n-p junction transistor.

Lead connections are made by fastening soldering-lug connectors directly to the paper with eyelets and an eyelet punch, and then painting silver paste over the connector and paper. A scale of $\frac{1}{2}$ inch = 0.001 inch has been found convenient. The electrodes are connected in the usual bridge circuit (either ac or dc) with a suitable balance indicator and probe. The equipotential plot is obtained either by a pantograph or more simply by using carbon paper underneath the Teledeltos paper to record the lines along which balance is obtained.

Suppose one chooses to find the hole flow map with s = 5000 cm/sec. From Eq. (17) $aR = D_p p/s = 40 \times 2 \times 10^3/5 \times 10^3 = 16$. For maximum accuracy the boundary segments a should be as small as possible so as to most nearly approach

---
[8]Obtainable from Western Union Telegraph Co.

7

a continuous distribution. A value of $\frac{1}{2}$ to $\frac{1}{4}$ mil (1/4 – 1/8 inch on the model) leads to negligible error. Since this segment size would require hundreds of segments to cover the boundary, use is made of the fact that for s constant only the product aR need be fixed over the boundary. Hence, a is chosen to be smallest on that region of the boundary along which the potential is changing most rapidly, or in other words, where the tangential component of ∇P is largest. Then the suitable value of R is chosen. For example, experience shows that the region near the intersection of the emitter electrode and the surface requires $a = \frac{1}{2}$ mil ($R = 12600$ ohms), while for the boundary at the edge of the wafer, $a = 3$ mils ($R = 2100$ ohms) will suffice. A simple and convenient way to obtain varying segment lengths is to draw the boundary as a continuous conducting line, then cut it into segments with a razor blade.

When the equipotential map has been obtained, the field lines or hole flow lines are drawn in using the method of rectilinear squares.[4] The map of Fig. 3a results. It should be noted that although equipotential lines are normal to flow lines, the equipotentials do not intersect the free surfaces of the germanium at right angles when $s > 0$. In fact it is just this departure from normal incidence which accounts for the flow of holes into the surface.

To calculate β, the current density must be integrated across the emitter surface to give

$$\beta = \frac{\text{that part of the total current which leaves the emitter and arrives at collector}}{\text{total current leaving emitter}}$$

This is easily done by drawing a scale along the emitter radius as in Fig. 3, and multiplying the number of tubes of flow leaving the emitter per small increment in r, by r, and summing over r. In the example chosen $\beta = 79/89 = 0.89$. Arbitrary units are used here since the final quantity β is dimensionless.

Fig. 3b shows the map obtained with emitter and collector reversed. Then $\beta = 0.38$.

Results

A. Test of Segmentation

To test whether the finite segmentation of the boundary introduces of itself an error into the flow map, two models were prepared with
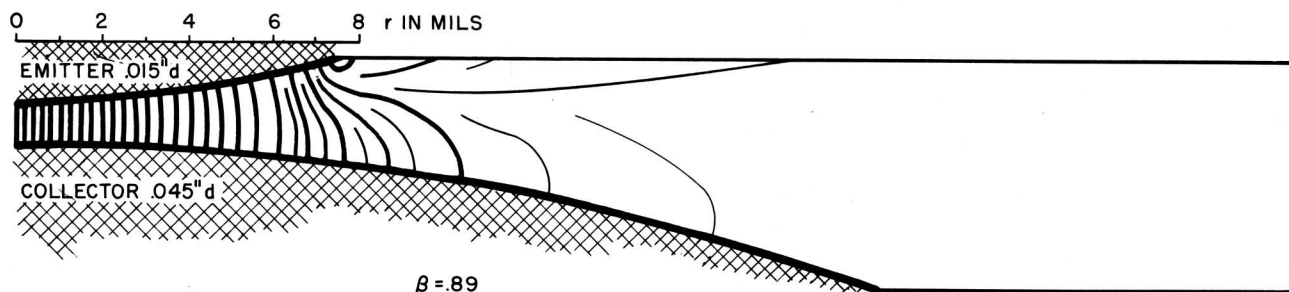

$\beta = .89$

Fig. 3a – Hole Flow Map
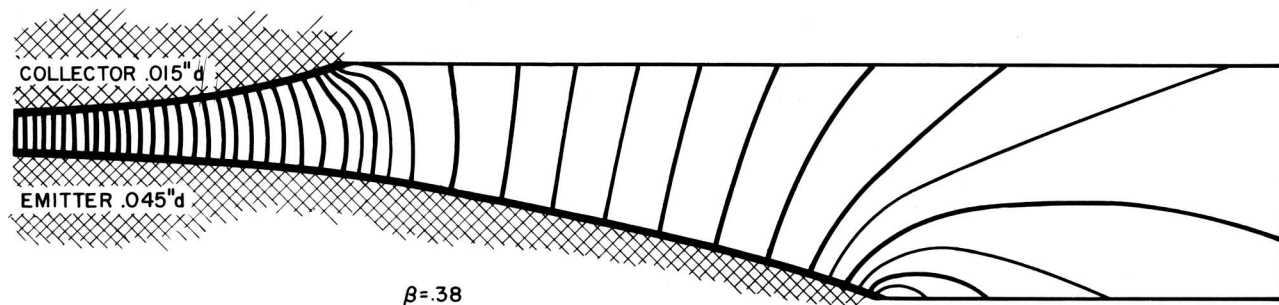TA–153 Geometry
S = 5000 cm/sec.

$\beta = .38$

Fig. 3b – Hole Flow Map
TA–153 Geometry – emitter and collector interchanged
S = 5000 cm/sec.

spherical emitter and collector, as in Fig. 3. One had no conducting strips on the boundary. The other had the boundary segmented according to the principle of maximum tangential gradient as described above, but the segments were not connected back to ground. Thus in this case $R = \infty$, $s = 0$. The validity of the segmentation method was evidenced by the fact that the two maps were almost identical. In small regions near the edge of a few segments there was a sudden shift in the equipotential lines which did not correspond to the same equipotential in the unsegmented model. Decreasing the segment size in that particular region improved the map.

B. Effect of Emitter-to-Collector Area Ratio

It was recognized early in the alloy-transistor development that the use of larger collector than emitter diameters resulted in consistently higher values of α. Fig. 4 shows the results of experiments made to test this observation. Because of the unavoidable variance in this type of data taken on different units, each of the experimental points represents the average of a group of transistors with the same nominal emitter/collector area ratio. The surfaces were etched or otherwise treated in the same manner after the junction had been formed. α approaches unity as collector/emitter area ratio gets larger. This curve illustrates the improved collection efficiency obtained by enlarging the collector diameter.
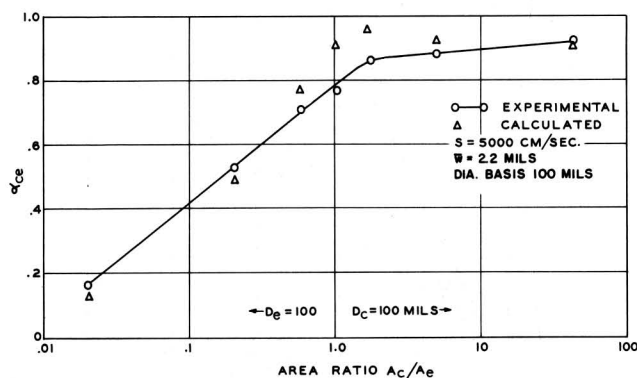

Fig. 4 — Dependence of α_{ce} on collector-emitter area.

In order to gain a more quantitative insight into this design parameter, a series of hole flow maps was made using emitter and collector diameters within the range covered by the above experiment. After some preliminary trials, a value of $s = 5000$ cm/sec was chosen

as that required to get the best fit to the data. The calculated curve of α vs area ratio is also shown in Fig. 4. The sensitivity of α to s is such that had s been taken as 3000 cm/sec the calculated curve would have fallen wholly above the data, while for $s = 10,000$ cm/sec the curve would have been wholly beneath the experimental results. With $s = 5000$ cm/sec, the calculated α fits the data well at low and high values of area ratio, but shows a marked departure near ratio = 1. In fact, the computed curve gives a broad maximum near ratio 1:2; this maximum was absent in the experimental results.

The maximum in the calculated curve comes about in the following way: Consider the collector diameter fixed. With a small emitter, collection is very efficient. There is little loss to the surface near the collector, while most of the holes are lost near the edges of the emitter. As the emitter is made somewhat larger the loss of holes to the surface near the emitter increases roughly as the perimeter, but the total hole injection increases as the area. The loss near the collector is still negligible. The net result is that α rises slowly. As emitter diameter approaches and exceeds collector diameter, hole loss to the surfaces near the edges of the collector increases very rapidly, dominating all other hole losses. Then α decreases rapidly.

The experiment was repeated, using somewhat different emitter and collector diameters, but covering roughly the same range of area ratios. Near ratio = 1 the axial alignment of emitter and collector is very critical. Using improved carbon jigs (see *LB-868*) the data of Fig. 5 were obtained. New hole flow maps covering this geometry were made with results indicated in the figure. Again using $s = 5000$
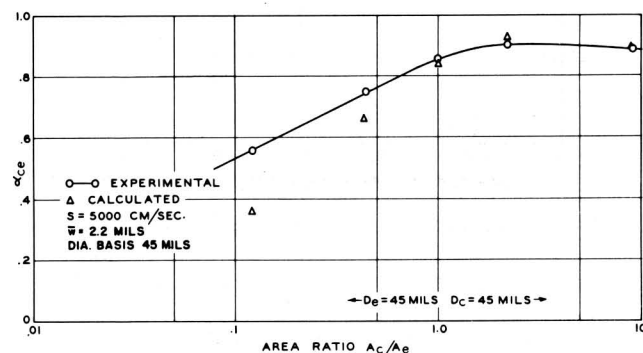

Fig. 5 — Dependence of α_{ce} on collector-emitter area.

cm/sec, a good fit was obtained for area ratios 10 down to 1, including the maximum predicted above. Below area ratio 1 the calculated curve deviates from the experiment. It is not known whether etching variables contributed to this disagreement. Variations in the shape of the alloy junctions from the assumed spherical form may also play a part. This aspect will be discussed later. Yet the general nature of the curve is reproduced well by the plotting method. The maximum in α is broad enough, so that for practical purposes a choice of area ratio from 2 to 9 is satisfactory. A high ratio allows a greater emitter-collector misalignment tolerance.

C. *Variation of α with s for Plane Alloy Junctions*

The effect of s on α is shown in Fig. 6 in which s is taken as a parameter for α_{ce} vs junction diameter, d. In this case, equal diameter, plane parallel junctions were used at a fixed spacing of 1 mil but edge effects were included. Under the assumptions made in the solution, neglect of edge effects results in $\alpha_{ce} = 1$ for all d and s. Similarly, if $s = 0$, $\alpha_{ce} = 1$ for all d even with edge effects. The latter condition is shown as a dotted line in the figure. As d gets larger, all curves approach $\alpha_{ce} = 1$ asymptotically since the edge effects become of little importance.
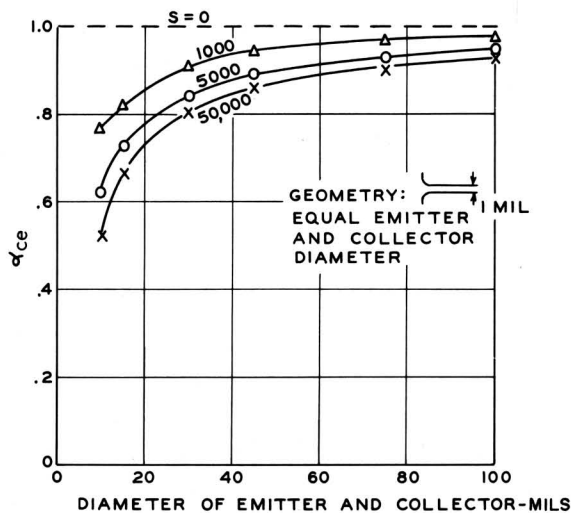

Fig. 6 – Dependence of α_{ce} on junction diameter.

The same information, plotted in terms of α_{cb} instead of α_{ce} ($\alpha_{cb} = \frac{\alpha_{ce}}{1-\alpha_{ce}}$) is shown in Fig. 7. The interesting fact is that α_{cb} is

directly proportional to d for this geometry. This can be understood by the use of an argument similar to that used to explain the maximum in Fig. 4. The collector collects holes in proportion to its area. The emitter region must be divided into two parts. The central section emits proportionally to area. The perimeter region, because of the high gradient of P concentrated there, emits proportionally to perimeter length πd.

Let $\alpha_{ce} = \dfrac{\text{collector current}}{\text{emitter current}} = \dfrac{K_1 d^2}{K_2 d^2 + K_3 d}$

It is known that $\lim_{d \to \infty} \alpha_{ce}$ must be 1, hence $K_1 = K_2$.

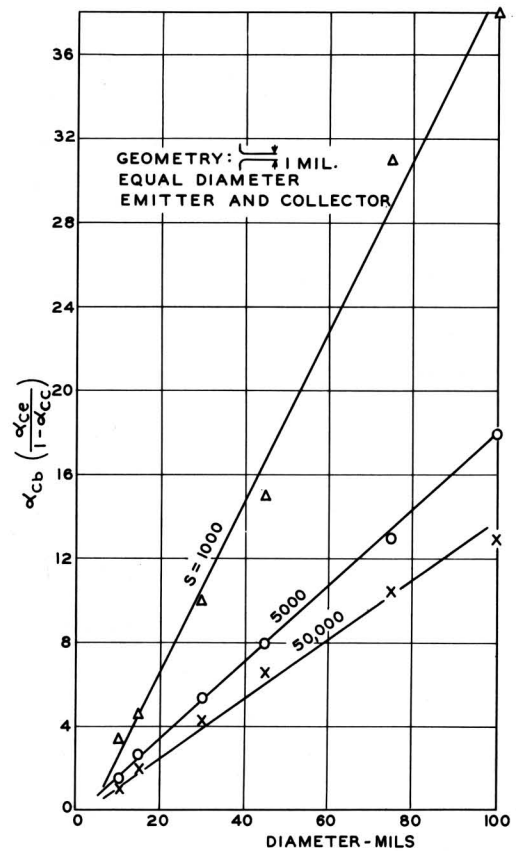Then $\alpha_{cb} = \dfrac{\alpha_{ce}}{1-\alpha_{ce}} = \dfrac{K_1}{K_3} d.$

Fig. 7 – Dependence of α_{ce} on junction diameter.

D. *Comparison of Plane and Spherical Junctions*

A direct comparison was made of plane parallel alloy junctions with edge effects and spherical alloy junctions with the same diameter of emitter and collector. The value of s

d the minimum spacing were the same for both .ses. α_{ce} was 0.92 for the spherical case and 0.97 for the plane case, and α_{cb} was 11 and 32, respectively. The advantage of the plane junction is clear. As a further comparison, a grown junction geometry was computed, again for the same s and W. A value of α_{ce} = 0.97 and α_{cb} = 32 was obtained. Hence, grown parallel junctions and alloy parallel junctions are comparable. Of course, this assumes perfect emitter efficiency. This is less likely for the grown junction. Comparison of curved and plane junctions on a frequency basis will be made in a subsequent section.

E. *The Absolute Value of s*

The curves of Figs. 4 and 5 were calculated in order to show that the general form of α vs area ratio can be predicted by the plotting method neglecting volume recombination. The choice of s = 5000 cm/sec may be open to question, however. Surface recombination velocity has been measured on germanium bars by independent methods in various laboratories[7]. Table II summarizes the results.

Table II

Treatment	s
Sandblast	$10^4 \cdot 10^5$ cm/sec
Chem. etched	2×10^3 to 4×10^2, depending on specific etch.
Electrolytic etch	2×10^2

None of these measurements was made in transistor structures. All measurements on etched germanium are very sensitive to etching conditions, freshness of solution, etc. If it is assumed that the etching processes carried out in the presence of indium during fabrication of the transistor are the same as those on germanium bars, the assumed value of s = 5000 cm/sec appears somewhat high. Because of the variations in surface treatment, alloying rate, and electrode centering likely during mall scale fabrication of the special units sed for the area ratio tests, an estimate of s was attempted using only TA-153 units processed according to a set practice (see *LB-868*). Even under these conditions, experience indicates that there are variations in junction shape and

[7]See Conwell, "Properties of Silicon and Germanium", *Proc. I.R.E.*, Vol. 40, p. 1335, (1952).

minimum spacing which could influence an absolute determination. However, hole flow maps show that the ratio of α_{ce} in the normal connection, α_N, (0.015" emitter, 0.045" collector) to α_{ce} in the inverted connection, α_I, (0.045" emitter, 0.015" collector) is less sensitive to junction shape than either α_N or α_I separately. The average base layer thickness, $\overline{W}$, can be estimated from emitter input capacitance, since this capacitance arises chiefly from diffusion of holes through the base layer. Hence, a sample of 38 TA-153 transistors were selected with $\alpha_{N_{ce}}$ >0.95 and average spacing, $\overline{W}$, of 2.2 ± 0.2 mils. The value of α_N / α_I was 1.41 ± 0.1. Fig. 8 shows a calibration curve obtained by hole mapping in which α_N / α_I is plotted against s for 2.2 mil average spacing (1 mil minimum assuming spherical geometry). From the curve, it is estimated that s = 460 cm/sec. This value is in the range shown in Table II for chemical etching.
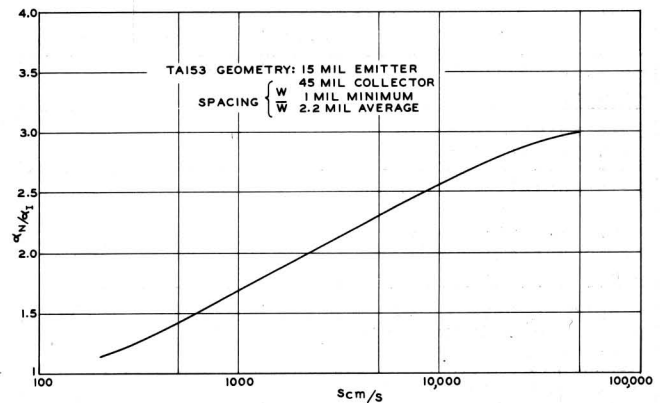

Fig. 8 – α_N / α_I vs surface recombination velocity s.

Another sample of 15 transistors was selected with α_N<0.9 and the same base layer thickness as before. The value of α_N / α_I was 2.09 ± 0.2, giving s = 3000 cm/sec. It appears that many cases of low α can be ascribed to improper surface treatment.

It must not be assumed, however, that all low α units are the result of high s. The search for the low α sample above disclosed many transistors with α_N / α_I >3, which usually turned out to be due to large base thickness. The calibration curve of Fig. 8 applies only to the 2.2 mil average base thickness. Larger thicknesses could be calculated. They would yield similar curves lying above the present curve, so that for a given s α_N / α_I increases as

W and $\overline{W}$ increases. This is an important point which argues in favor of three-dimensional theory without volume recombination. If a one-dimensional theory with volume recombination dominant over surface recombination were applicable, α_N/α_I would be independent of W.

The calibration curve of Fig. 8 can also be used to follow changes in s due to various surface treatments on the same transistor. To illustrate this application, a group of unpotted transistors was made up from which three units were selected which had average base thicknesses of 2.2 mils. They were then treated with various solutions. After each treatment the units were washed in distilled water, dried, and α_N/α_I measured. The corresponding value of s was then obtained from Fig. 8. Typical data were as follows:

Table III

TA-153 Geometry, Unit A_2			
Treatment	α_N/α_I	s	α_{cbN}
Standard TA-153 etching[a]	1.35	400 cm/sec	24
Electrolytic etch in 1% NaOH solution	1.16	200	37
Etch containing $Cu(NO_3)_2$.[a] Etch for 10 sec. Very slight deposit of copper on the Germanium	2.41	7400	0.7
Copper removed by Ammonia and Hydrogen Peroxide solution	1.20	250	30
Distilled water which had been boiled with a piece of brass[a] after 5 min. after 10 min. after 3 hours	1.13 1.11 2.5	180 150 10000	28 52 0.5
Electrolytic etch in 1% NaOH	1.25	280	27
Saturated solution of $ZnCl_2$	1.64	880	9
Electrolytic etch in 1% NaOH	1.20	250	32

It can be seen that surface treatment vary s over wide limits. Yet the processes are quite reversible; electrolytic etching always restores the surface approximately to $s = 250$ cm/sec.

The significance of surface recombination velocity in device performance and the ease with which s may be measured suggest that the method may have application as a quality control test in junction transistor manufacture.

F. Transit-Time Dispersion

The properties of junction transistors at the higher frequencies depends on many factors such as diffusion time through the base layer (diffusion capacitance), junction capacitance of the collector, internal lead resistance, etc. These have been discussed in the literature[1]. Because transistor theories have been confined to one-dimensional analyses, the factor of transit time spread due to path length variation has been ignored. This type of dispersion is similar to the path-length--transit-time effect in electron multiplier tubes, wherein electrons which have traversed various paths through the multiplier have spread in transit time. This dispersion has been calculated for the TA-153 structure, using the hole flow map to estimate the path length distribution. Then, since $t = x^2/D_p$, the relative number of holes having transit times between t and $t + \Delta t$ is obtained. An analysis of this dispersion curve indicates that α_{ce} will be down 3 db at about 1 Mc due to this effect. A similar calculation in a plane parallel alloy structure including edge effects shows that α_{ce} is 3 db down at 5 Mc. While at present the other limits to high-frequency performance in the TA-153 are more important, future design of special high-frequency transistors should take the path-length dispersion into account. This can be done by attempting to provide parallel junctions.

Jacques I. Pankove

Arnold Moore

[a] See Navon, Bray and Fan, "Lifetime of Injected Carriers in Germanium", *Proc. I.R.E.*, Vol. 40, p. 1345, (1952). The values of s given in this reference are not in conflict with the present results because the etching conditions were different. The presence of indium on the germanium causes a slight deposition of copper which apparently greatly increases surface recombination.